PAPER

Check for updates

Structural properties and antioxidation activities of lignins isolated from sequential two-step formosolv fractionation†

Xiaoxia Duan,[ab] Xueke Wang,‡[a] Jiangwei Chen,[a] Guijiang Liu[a] and Yun Liu [ID] *[a]

In order to investigate the solubility behavior of lignin in formic acid (FA) solution *Phragmites australis* biomass was subjected to a sequential two-step formosolv fractionation using 88% FA followed by 70% FA to obtain four specific lignin fractions, designated as IFL-88%, IFSL-70%, IFIL-70% and IFL-EtAc. The structures of the four isolated lignin fractions were successfully characterized by gel permeation chromatography (GPC), Fourier transform infrared (FTIR) spectroscopy, two-dimensional heteronuclear single quantum coherence nuclear magnetic resonance spectroscopy (2D-HSQC NMR), thermogravimetric analysis (TGA), and gas chromatography-mass spectroscopy (GC/MS). Furthermore, the total phenolic content of the four isolated lignin samples was assessed by Folin-Ciocalteu analysis. The data from structural properties revealed that depolymerization of the isolated lignin fractions occurred *via* β-O-4 cleavage, accompanied by competitive condensation reaction. Interestingly, 70% aqueous FA could separate specific lignin fractions with different antioxidant capacities of ABTS·+ and DPPH radical scavenging activity. Due to the high total phenolic hydroxyl content (25%) and low molecular weight (Mw = 2760 Da) and polydispersity index (PDI = 1.5), IFL-EtAc lignin showed excellent antioxidant activity at the same concentration of 2.0 mg mL^{-1} in comparison with three other isolated lignin fractions, and it was even equal to that of commercial antioxidant butylated hydroxytoluene (BHT). These findings are helpful to separate specific lignins with higher value as potential antioxidants by sequential two-step formosolv fractionation in lignin chemistry.

1 Introduction

Lignin, consisting of guaiacyl (G), syringy (S) and *p*-hydroxybenzyl (H) subunits, is rich in aromatic structure, and has been widely viewed as a potential promising natural antioxidant.[1] The content of total phenolic hydroxyl groups and low molecular mass of the technical lignin is greatly responsible for the effective antioxidant activity.[2,3] In this case, a suitable fractionation process is essential for obtaining specific structural lignin fractions. Recently, formosolv fractionation has been proved to be a simple and economically viable approach for lignin isolation from lignocellulosic biomass.[4–10] For instance, our team previously isolated technical lignin from *Eucalyptus* biomass by 70% aqueous formic acid (FA) fractionation, and 73.18% technical lignin was obtained with a molecular mass weight (Mw) of 2582 g mol^{-1}.[5] Zhang and co-workers used 88% FA to separate

lignin from corn cob, and the isolated lignin had high molecular weight due to condensation reaction during FA treatment.[6] Li and co-workers reported a mild two-step pretreatment using anhydrous FA and alkaline hydrogen peroxide aqueous solution to separate lignin from bamboo, and the obtained lignin fraction showed a slight reduction of the molecular weight and a polydispersity of around 2.[7] Suriyacha and co-workers separated lignin from sugarcane bagasse using 10–30% FA-catalyzed organosolv process.[8] The use of aqueous FA in organosolv could increase the rate of cleavage of α- and β-ether linkages in lignin and resulted in the dissolution of lignin fragments with lower molecular weights.[7,8] Jin and co-workers investigated one-step fractionation with 99% FA at elevated temperatures with short retention time to achieve high guaiacyl lignin fractions from corn stover.[9] Qiao and co-workers proposed two-step pretreatment with FA (88%) followed by alkaline salt solution at room temperature for efficient removal of lignin from corncob.[10]

In regards of FA fractionation process of lignocellulose biomass, it is generally considered that FA not only acts as solvent reagent and acid-based catalyst, but also it seems to react with lignin to generate formate esters.[5,8,11] However, Halleraker and co-workers convinced that carbon from the FA incorporated in the carbonyl structures of the depolymerized

[a]*Beijing Key Laboratory of Bioprocess, College of Life Science and Technology, Beijing University of Chemical Technology, Beijing 100029, China. E-mail: liuyun@mail.buct.edu.cn; liuyunprivate@sina.com; Fax: +86-10-64416428; Tel: +86-10-64421335*
[b]*Beijing Zest Bridge Medical Technology Inc., Beijing 100176, China*

‡ The author (Xueke Wang) is equal contributor to this work.

lignin bio-oil to form carboxylic acids, not a result of a formylation reaction between lignin and FA.[12]

The tailor-made lignin fractions from lignocellulose showed various practical applications related to their structural properties. Lignin fraction with high heating value could be applied for thermochemical conversion purposes.[13] Lignin fraction enriched with β-O-4′ group would be an ideal candidate for production of aromatic monomers.[14] Lignin fraction with low molecular weight (Mw) was potential promising for non-fuel products in polymeric materials.[15] Lignin fraction with higher Mw and cross-linked structure was suitable for the catalytic oxidative/reductive fragmentation to produce fuel, pharmaceutical precursors and chemicals.[13,16] Lignin fraction enriched with reactive groups, including phenolic hydroxyl, methoxyl, aliphatic hydroxyl and double bond in the side chain, can be used as an efficient antioxidant.[17]

In order to shed light on the direct relationship between lignin structural properties and its antioxidant activity, in this present study, a sequential two-step formosolv fractionation of *Triarrhena lutarioriparia* biomass is proposed to obtain four specific lignin fractions with different solubility in FA solution. As a native potential C_4-plant, *T. lutarioriparia* grows well in wet environments, it is plenteous along Tongting Lake with the output of 920 000 tons per year in Hunan province, China. The objective of this present work is to isolate specific lignin fraction with high antioxidation capacity from *T. lutarioriparia* by sequential two-step formosolv fractionation processes using 88% FA as solvent followed by 70% aqueous FA. The isolated lignin fractions are characterized by Fourier transform infrared (FTIR) spectroscopy, gel permeation chromatography (GPC), thermogravimetric analysis (TGA), and two-dimensional heteronuclear single quantum coherence nuclear magnetic resonance (2D-HSQC NMR) techniques. The aromatic monomers derived from depolymerized lignin are also qualitatively determined by gas chromatography-mass spectroscopy (GC/MS). The total phenolic content (TPC) is determined by Folin-Ciocalteu (FC) assay. The antioxidant activities of all four lignin fractions were monitored with DPPH and ABTS$^{\cdot+}$ radical scavenging activity using UV-VIS spectroscopy method. Based on the experimental data, this paper aims to explore the straightforward correlation between the structural characteristics and its antioxidant activity of the specific lignin fractions through sequential two-step formosolv fractionation.

2 Materials and methods

2.1 Materials

T. lutarioriparia biomass used as a feedstock was kindly provided by Hunan Agricultural Science Academy (Changsha City, China). The biomass was irradiated at the dose of 400 kGy according to the method reported in our previous work.[18] The irradiated biomass was ground by a high-speed grinder and screened to the particle sizes of 40 mesh (*i.e.*, 0.4 mm). The contents of cellulose, hemicellulose and lignin in biomass feedstock were determined to be approx. 38%, 17% and 29%, respectively, which was measured according to standard procedure in National Renewable Energy Laboratory (NREL) (**http://www.nrel.gov/biomass/analytical_procedures.html**). Deuterated chloroform ($CDCl_3$), anhydrous pyridine, and dimethyl sulfoxide-d6 (DMSO-d6) were purchased from Sigma-Aldrich. Other reagents and solvents were purchased from Aladdin Co., Ltd. (Shanghai, China) and used directly without further purification.

2.2 Sequential two-step formosolv fractionation and lignin fraction preparation

Scheme 1 shows the procedure flow of the sequential two-step formosolv fractionation using 88% FA followed by 70% aqueous FA for lignin fraction preparation from *T. lutarioriparia* biomass.

In brief, *T. lutarioriparia* biomass was irradiated at the dose of 400 kGy according to the method reported in our previous work,[18] the reason why the biomass was irradiated is the fact that irradiation treatment could damage the stubborn structure of biomass so that lignin would be dissolved in FA solution.[5] The irradiated biomass was crushed and screened to 40 mesh. 500 g of the pretreated powder biomass were mixed with 5 L of 88% FA (mass/volume ratio of solid to liquid was set 1 : 10). The mixture was reacted at 100 °C and 280 rpm for 3 h. After reaction completion, the mixture was filtrated and washed with 88% FA three times. The liquor from filtration and washing was combined and then evaporated at 70 °C in vacuum to recover FA, the recovery efficiency of FA was calculated over 90% in our experiments. Until the total volume of liquor was approx. 50 mL, 500 mL deionic water was added to precipitate lignin. Through centrifugation, the solid residue was washed with water to completely remove FA and then dried in oven at 80 °C to obtain the
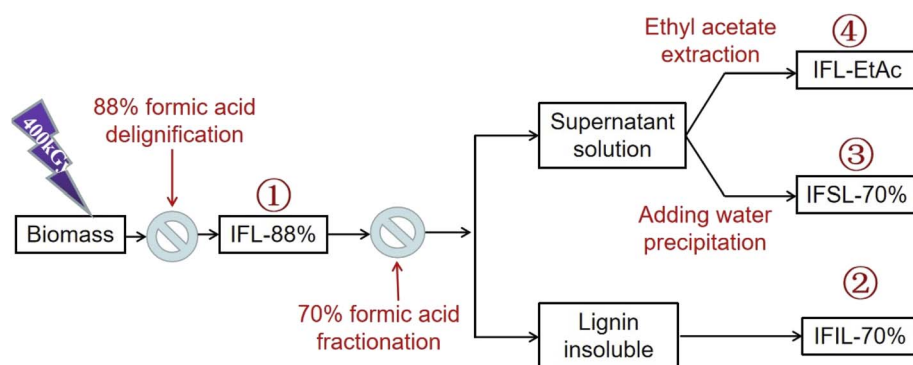
Scheme 1 Overview of lignin preparation *via* sequential two-step formosolv fractionation.

precipitated lignin, which was denoted as IFL-88% (~39 g, purity of 94%). Subsequently, the resultant IFL-88% lignin fraction (5 g) was dissolved in 70% FA solution (500 mL) with the mass/volume ratio of 1 : 10 and stirred at 100 °C for 3 h. After reaction, the supernatant and the insoluble lignin were separated by centrifugation, the insoluble lignin was washed with deionic water several times to completely remove FA until the solution was neutral. The insoluble lignin fraction obtained from 70% FA fractionation was denoted as IFIL-70%, which was dried in oven at 80 °C and stored in a 50 mL vial for analysis. The supernatant was treated in two ways. In one way, the supernatant was rotary evaporated to the total volume of approx. 50 mL, and then 500 mL water was added to precipitate lignin. This lignin fraction was named as soluble lignin in 70% FA solution and denoted as IFSL-70%. After centrifugation and dried in oven at 80 °C, IFSL-70% was obtained. In another way, when the supernatant was rotary evaporated to the total volume of approx. 50 mL, it was extracted with ten-fold ethyl acetate (EtAc). After recovery of EtAc, lignin fraction extracted by EtAc was obtained and denoted as IFL-EtAc fraction.

2.3 Characterization of the isolated lignin fractions

2.3.1 GPC analysis. Due to poor solubility, lignin fractions were acetylated with pyridine/anhydride (1 : 2, v/v) prior to GPC analysis, which procedure was detailed in ref. 19. The acetylated lignin dissolved in tetrahydrofuran (THF) was performed on GPC equipment (Agilent 1260, USA) with a PLgel 15 μm MIXED-E column (Agilent, USA) for average molecular weight and molecular weight distribution. THF was used as the mobile phase with the flow rate of 1 mL min^{-1}. The internal standard was polystyrene (Sigma-Aldrich) with different molecular weights (Mw = 580, 1920, 4750, 9570, 27 810 Da).

2.3.2 FTIR spectroscopy analysis. FTIR experiments were conducted to reveal the functional groups of the isolated lignin fractions. Briefly, approx. 1 mg of the dried lignin powder and 100 mg of dried potassium bromide (KBr) was uniformly mixed and pressed into slice, which was tested on a Bruker TENSOR 27 FTIR spectroscopy (Bruker, Germany). Ten scans for each sample were taken with a resolution of 0.5 cm^{-1} ranging from 400 to 4000 cm^{-1}.

2.3.3 2D-HSQC NMR spectroscopy analysis. The accurately detail structural information of the isolated lignin samples was characterized by 2D-HSQC NMR (400 MHz, Bruker, Germany) at 25 °C.[20] Specifically, 60 mg of the acetylated lignin was dissolved in 500 μL of dimethyl sulfoxide (DMSO-d6) and placed into a 5 mm NMR tube for NMR analysis. The NMR assay conditions were: The number of acquisition points was 2048 and 256 for 1TD and 2TD, respectively. The scanning time (NS) was 64, the spectrum width (SW) was 15.9794 ppm (with 1SW and 2SW values of 259.9935 and 15.9794 ppm, respectively), and the center frequencies were 4.7 and 100 ppm for O1P and O2P, respectively.

2.3.4 GC/MS analysis. The aromatic monomer compositions in IFL-EtAc lignin fraction was qualitatively determined on a Trace ISQ GC/MS System from Thermo Fisher Scientific Co. (Waltham, MA, USA) with TR-WAXMS capillary column (30 m × 0.25 mm × 0.25 μm).[21] GC analysis conditions were: split ratio was 1 : 10, injector temperature was 250 °C, gas flow rate was 1

mL min^{-1} and GC oven temperature program were applied: 40 °C for 1 min, followed by a heating rate of 15 °C.min^{-1} from 40 °C to 250 °C and retaining at 250 °C for 10 min. MS analysis conditions were: Inter phase valve delay was set to 5 min, MS detector was EI source with ion-source temperature of 250 °C. MS scans were from 33 amu to 500 amu. Compounds were identified using the ChemStation software and the Replib library.

2.3.5 TGA measurement. The thermal stability of the isolated lignin samples was performed on A TGAQ50 thermal gravimetric analyzer (TA instruments, USA). Approx. 5 mg of the lignin samples pre-vacuum-dried at 40 °C for 48 h were heated from room temperature to 800 °C at a heating rate of 10 °C min^{-1} under nitrogen atmosphere.

2.3.6 Determination of total phenolic content (TPC). The total phenolic content (TPC) of the isolated lignin fractions was determined by Folin-Ciocalteu (FC) method based on a redox reaction using gallic acid as ref. 22. TPC was expressed as gallic acid equivalents (GAE), calculated from a calibration curve with six different concentrations (0, 0.02, 0.04, 0.06, 0.08 and 0.10 mg mL^{-1}) of gallic acid dissolved in DMSO. TPC of the lignin fraction was calculated by eqn (1):

$$\text{TPC} \ (\%) = \frac{\text{GAE} \ (\text{mg L}^{-1})}{\text{concentration of lignin} \ (\text{mg L}^{-1})} \times 100\% \quad (1)$$

2.4 Antioxidant activity of the isolated lignin fraction

2.4.1 ABTS$^{\cdot+}$ radical scavenging assay. The ABTS assay was performed at 734 nm on a UV-Vis spectroscopy (Youke Co., Shanghai, China) according to the method reported in the literature.[23] Briefly, 7.4 mM ABTS stock solution was reacted with 2.6 mM potassium persulfate solution, leading to the form of the ABTS radical cation (ABTS$^{\cdot+}$) after standing for 12–16 h at 25 °C in a dark place. Then, the obtained ABTS$^{\cdot+}$ solution was diluted with ethanol to the absorbance of 0.7 at 734 nm, and equilibrated at 25 °C. Lignin sample dissolved in ethanol (40 μL) was mixed with 4 mL of the ABTS$^{\cdot+}$ solution and incubated for 30 min in the dark. Ethanol solution was as the blank control. The absorbance was recorded at 734 nm, and all measurements were performed in triplicates. The ABTS$^{\cdot+}$ radical scavenging activity was calculated by eqn (2) using commercial antioxidant, BHT as the positive control. The calculated IC$_{50}$ value represented the concentration inhibiting 50% of the initial ABTS$^{\cdot+}$ radical.

$$\text{ABTS}^{\cdot+} \ \text{radical scavenging activity} \ (\%)$$
$$= \frac{A_{\text{control}} - A_{\text{sample}}}{A_{\text{control}}} \times 100\% \quad (2)$$

where A_{control} and A_{sample} are the absorbance at 734 nm of the blank control and lignin sample, respectively.

2.4.2 DPPH radical scavenging activity assay. The DPPH radical scavenging assay was measured at 517 nm on a UV-Vis spectroscopy (Youke Co., Shanghai, China) according to the method reported by Wei *et al.*[24] Briefly, 0.6 mmol L^{-1} of DPPH solution was prepared with ethanol and stored at 4 °C in a dark place. Lignin sample solutions with concentrations of 0.1, 0.2, 0.3, 0.4, and 0.5 mg mL^{-1} were prepared in 90% aqueous dioxane solvent. Subsequently, a 200 μL aliquot of lignin sample

solution was added into 4.3 mL of ethanolic DPPH solution, and the mixture was incubated at room temperature for 30 min in the dark. Ethanol solution was used as the blank control. The concentrations of DPPH radicals at 0 and 30 min were monitored at 517 nm. All experiments were repeated in triplicates. The DPPH radical scavenging activity of lignin fraction was calculated by eqn (3). The calculated IC_{50} value represented the concentration inhibiting 50% of the initial DPPH radical.

$$\text{DPPH radical scavenging activity } (\%)$$
$$= \frac{\text{absorbance}_{t=0 \text{ min}} - \text{absorbance}_{t=30 \text{ min}}}{\text{absorbance}_{t=0 \text{ min}}} \times 100\% \quad (3)$$

3 Results and discussion

3.1 Lignin solubility behavior in aqueous FA solution

Fig. 1 shows the balance of IFL-88%, IFIL-70%, IFSL-70% and IFL-EtAc lignin fractions with high purity of more than 94%. The yield of the aforementioned four lignin fractions was calculated as 29%, 61%, 17.1% and 19.7%, respectively. During the first-step 88% FA fractionation, lignin could dissolve in FA solution by acid-cleavage of α-aryl ether and aryl glycerol β-ether of lignin.[25] However, lignin soluble in 88% FA would lead to 61% insoluble precipitate in the second-step 70% FA fractionation. It indicated that low concentration of FA might deteriorate lignin solubility. In principle, solubility behavior of lignin in FA solution is a relatively obscure due to the complexity and heterogeneity of lignin structure. Ma and co-workers considered that solubility parameters of lignin in FA solution were largely dependent on lignin structure.[26] To date, lignin dissolving behavior in FA solution cannot be accurately described through the relationship between lignin structure and its solubility parameters.

3.2 Characterization of the isolated lignin fractions

It has been demonstrated that the antioxidant activity of lignin is associated with its molecular weight to some content.[24]

Therefore, GPC chromatographs were performed to determine the molecular weight of the isolated lignin fractions, and molecular weight-average (M_w), molecular number-average (M_n), and polydispersity index (PDI) are shown in Table 1. The traces of GPC analyses are provided in Fig. S1 in the ESI.†

For sequential two-step formosolv fractionation, depolymerization and condensation reactions were competitively realized. In comparison with IFL-88%, IFIL-70% shows the higher values of M_n and M_w (Table 1). It indicates that lignin condensation is probable the major reaction, leading to an obvious increase in M_w value from 7832 Da of IFL-88% up to 9907 Da of IFIL-70%, which is insoluble in 70% aqueous FA solution. Lignin condensation under acidic conditions primarily took place between the benzylic carbocations (Cα) of side chain and the electron rich nuclei of the aromatic ring.[27] However, IFSL-70% and IFL-EtAc show lower M_n and M_w in comparison with IFL-88%, hinting depolymerization reaction is in a dominant position in this case. Moreover, IFSL-70% and IFL-EtAc also have relatively smaller PDI than FL-88%. Lignin with smaller molecular weight and better homogeneity shows better solubility in organic solvents, which is of great help for further valorization.[15,24] When lignin molecular dissolves in aqueous FA solution, depolymerization reaction occurs to produce aromatic monomers with lower molecular weight.[28–30] However, the FA-induced depolymerization of lignin into lower mass molecular fractions could amend the solubility and mobility of lignin, thereby increasing the chance of their

Table 1 Molecular weight analyses of acetylated lignin samples by GPC[a]

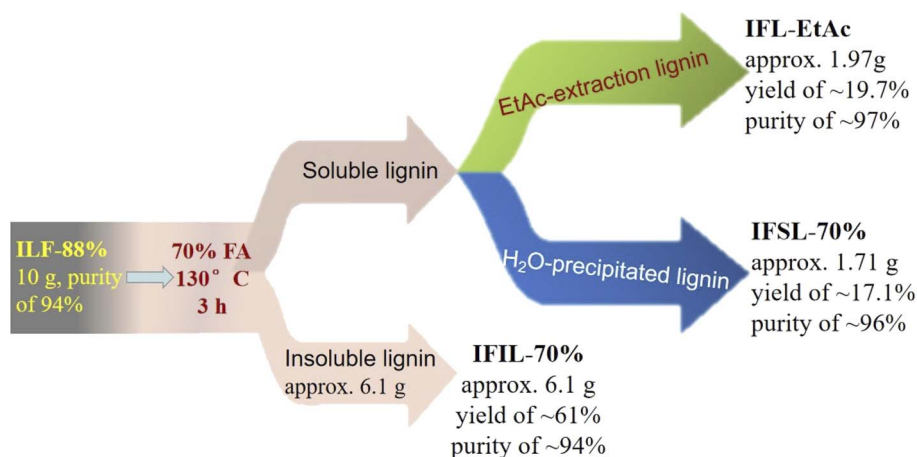| Trial	Lignin samples	M_n (Da)	M_w (Da)	PDI
1	IFL-88%	3013	7832	2.6
2	IFIL-70%	3632	9907	2.7
3	IFSL-70%	2006	3123	1.6
4	IFL-EtAc	1866	2760	1.5

[a] PDI: polydispersity index.

Fig. 1 The resultant lignin fractions obtained from sequential two-step formosolv fractionation.

condensation.[31] Therefore, sequential two-step formosolv fractionation had a significant influence on the molecular weight of lignin specimens.

The FTIR curves of the isolated lignin fractions obtained from sequential two-step formosolv fractionation are shown in Fig. 2a. According to the descriptions in the literature,[24,32,33] peak at 3426 cm^{-1} is ascribed to O–H stretching vibration in aromatic and aliphatic hydroxyl groups of the isolated lignin specimens. Peaks at 2935 cm^{-1} and 2843 cm^{-1} represent the C–H asymmetric and symmetrical stretching vibrations, originating from methyl (–CH$_3$), methylene (–CH$_2$–) and methine (–CH–) groups of lignin. The absorption peak at 1724 cm^{-1} refers to C=O stretching vibration. Aromatic skeleton stretching vibrations of lignin are observed at 1602 cm^{-1}, 1515 cm^{-1}, and 1427 cm^{-1}, while the absorption peak at 1457 cm^{-1} is the C–H asymmetric deformation vibration and aromatic vibration. Syringyl (S) units have absorption peaks at 1327 cm^{-1}, 1270 cm^{-1} and 1213 cm^{-1}, while 1120 cm^{-1} is associated with guaiacyl (G) units. Peak at 831 cm^{-1} is denoted as C–H out-of-plane in positions 2 and 6 of S unit and all positions of the *p*-hydroxyphenyl (H) units. FTIR results convince that G–S–H subunits are existing in the skeletal structure of lignin from *T. lutaioriparia*, although its real lignin structure is unknown so far. Observation from FTIR results, it is demonstrated that sequential two-step formosolv fractionation affects mainly on the variance of reactive functional group intensity of lignin, *e.g.* hydroxyl (–OH), methoxyl (–OCH$_3$) and carbonyl (C=O), does not change lignin skeletal structure.

Furthermore, the thermal stability of the isolated lignin fractions was characterized by TGA/DTG (Fig. 2b and c). As shown in Fig. 2b, three stages of the decomposition can be clearly identified in the TGA curves for all lignin samples. (I) An initial stage below 150 °C, the weight loss was attributed to the evaporation of the residual water in the lignin. (II) The main stage between 150 °C and 500 °C during which inter-unit linkages of the lignin breakup and monomeric phenols evaporate, leading to the major weight loss stage. (III) The final stage above 500 °C, the weight loss stage can be attributed to the decomposition of the aromatic rings of the lignin molecules.[34] After 800 °C, the residue mass of IFL-EtAc fractions is approx. 26%, while the residue weight of other three lignin fractions, IFL-88%, IFSL-70% and IFIL-70%, is approx. 35–40% after 800 °C. As seen in Fig. 2c, the maximum decomposition temperature (Tm) of the IFL-EtAc is 367 °C, slightly higher than that of IFSL-70% (366.8 °C), IFIL-70% (365.8 °C) and IFL-88% (345.7 °C). It was demonstrated that the thermal stability of lignin was highly associated with the frequency of β-O-4 linkages in the lignin polymers.[33,35] The higher thermal stability, the less frequency of the β-O-4 linkages.[33] Due to some β-O-4 linkages in lignin structure cleavage during the second step 70% formosolv fractionation, the content of β-O-4 linkages decreases in IFL-EtAc lignin fraction, leading to relatively higher Tm value. Jin and co-workers considered that the higher Tm value was mainly due to the higher purity of FL-EtAc lignin fraction which generated better resistance to thermal degradation.[36]
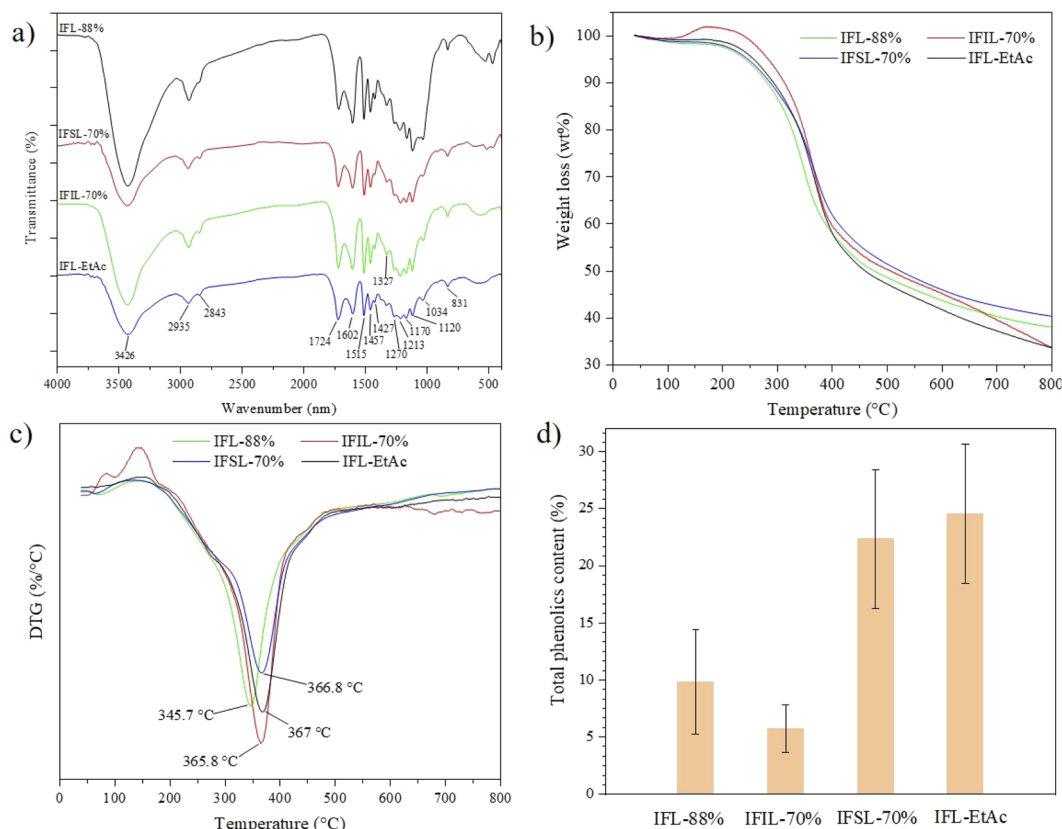

Fig. 2 Characterization of the isolated lignin fractions obtained from sequential two-step formosolv fractionation. (a) FT-IR curves; (b) TGA curves; (c) DTG curves; (d) total phenolic content (TPC) determination.
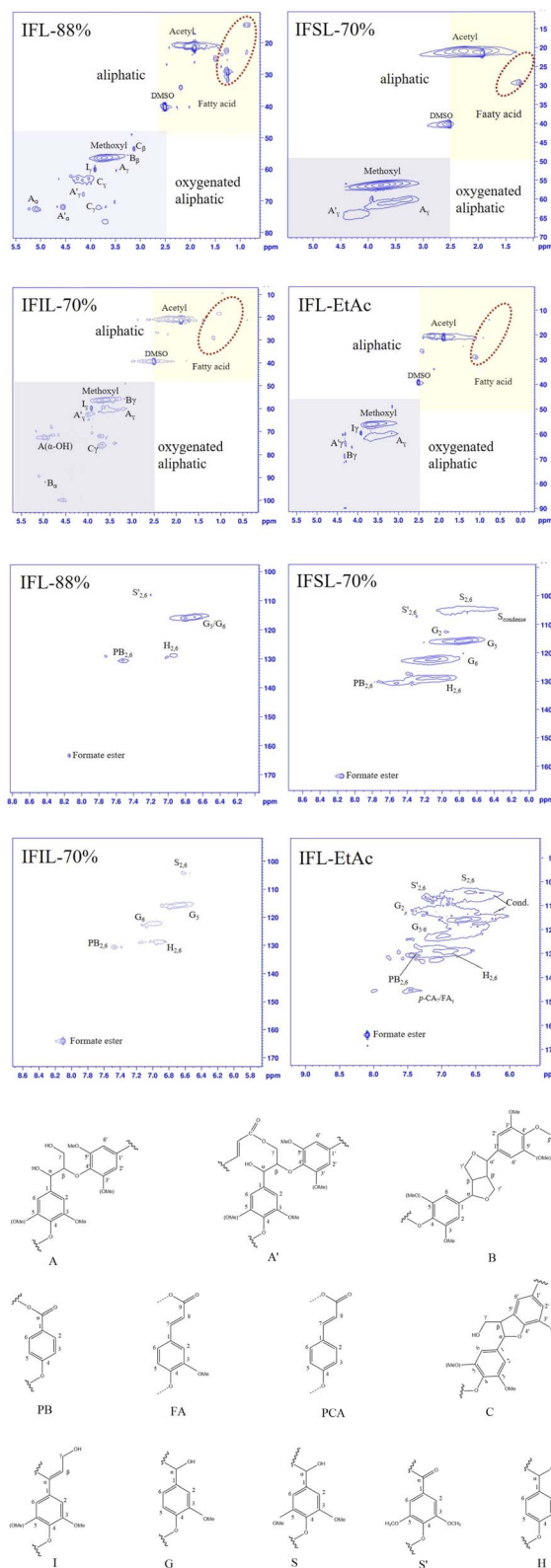
Fig. 3 Aliphatic regions (δ_C/δ_H 50–100/2.5–6.0) and aromatic regions (δ_C/δ_H 100–170/6.0–10.0) in the 2D-HSQC NMR spectra of the isolated lignin fractions obtained from two-step formosolv fractionation. The main structures of isolated lignins: (A) β-O-4′ structures, (A′) γ-acylated β-O-4′ substructures, (B) β-β′ resinol substructures, (C) phenylcoumarane substructures formed by β-5′ and α-O-4′ linkages, (I) phydroxycinnamyl alcohol end groups, (H) p-hydroxyphenyl units, (S) syringyl units, (S′) α-oxidized syringyl units, (G) guaiacyl units, (PA) p-hydroxybenzoate units, (PB) p-hydroxybenzoate units, (pCA) p-coumarate unites.

The TPC values for the isolated lignin fractions are analyzed by FC assay and the results are illustrated in Fig. 2d. It is noticeable that IFL-EtAc has the highest TPC value (~25%), following by IFSL-70% (~23%), IFL-88% (~10%) and IFIL-70% (~6%). García et al. reported that lignin soluble in acidic conditions should have a higher percentage of total phenols, because they contained few impurities and a high proportion of phenolic components resulting from cleavage of β-O-4 bonds.[8]

3.3 2D-HSQC NMR analysis of isolated lignin fractions

To further acquire more accurate details of the lignin structure, the isolated lignin fractions were characterized by 2D-HSQC NMR to reveal the aromatic units and inter-unit linkages in lignin. According to description in the literature,[33,37] the main substructures of lignin in the HSQC NMR spectra were assigned and the results are shown in Fig. 3. NMR spectra include aliphatic regions (δ_C/δ_H 5–100/0–5.5 ppm) and aromatic regions (δ_C/δ_H 100–170/6.0–8.5 ppm). In the top-right corner of the aliphatic region, signals originated from fatty acids were observed (δ_C/δ_H 15–30/0.5–2.5 ppm). In the aliphatic region of HSQC spectra, β-O-4 aryl ether linkages (A), Cγ-acetylated β-O-4 aryl ether linkages (A′), α-O-γ and γ-O-α linkages (B) are identified in the isolated lignin fractions. Signals of methoxyl groups (–OCH₃) are strongly intensive in HSQC spectra for all isolated lignin fractions. It is interesting to observe that only signal of Ar was observed, and the signal of A_α and A_β was not identified in the HSQC spectra. It indicates that FA can increase the rate of cleavage of α- and β-ether linkages of lignin.[8] Moreover, several previous works demonstrated the dehydration reaction at acidic condition resulted in the formation of unsaturated bond and the elimination of cross-signals of in A_α, A_β of HSQC spectra.[33,37]

In the aromatic regions, the typical units of guaiacyl (G), syringyl (S), and p-hydroxyphenyl (H) are observed in the HSQC NMR spectra, the results are consistent with these in FTIR analyses (Fig. 2a). As observed from Fig. 3, the peak intensity of G unit is much stronger than S unit. The reduction of signal strength of S unit is probably ascribed to the condensation reaction at C_5 or C_6.[37] Some non-canonical structures, such as ferulate (FA), p-hydroxybenzoate (PB) and p-coumarate (p-CA), are also observed in the HSQC NMR spectra (Fig. 3). These non-canonical units were also found in the lignin structure of corn, wheat straw and reed stover.[37–40] Cross-signals at around δ_C/δ_H 106.4/6.6, 112.0/6.7 and 120.5/6.6 ppm related to the $C_{2,6}$-position of condensed S units and C_2 and C_6-position of condensed G units were markedly observed in the HSQC NMR spectra of IFSL-70% and IFL-EtAc, which could be attributed to the condensation reactions of the lignin during the second step 70% FA fractionation process. The process of the formation of condensed C–C bonds is that lignin β-ether unit formed benzyl carbocation ions at acidic conditions, which are nucleophilically attacked by electron-rich aromatic rings.[27] In addition, the peak of C_2-position of G unit is not detected in IFL-88% and IFIL-70% fractions, indicating the condensation reaction easily occurred at G units rather than S units.[41,42] Cross-signals at around δ_C/δ_H 161.9/8.2 ppm are assigned to the formate ester,
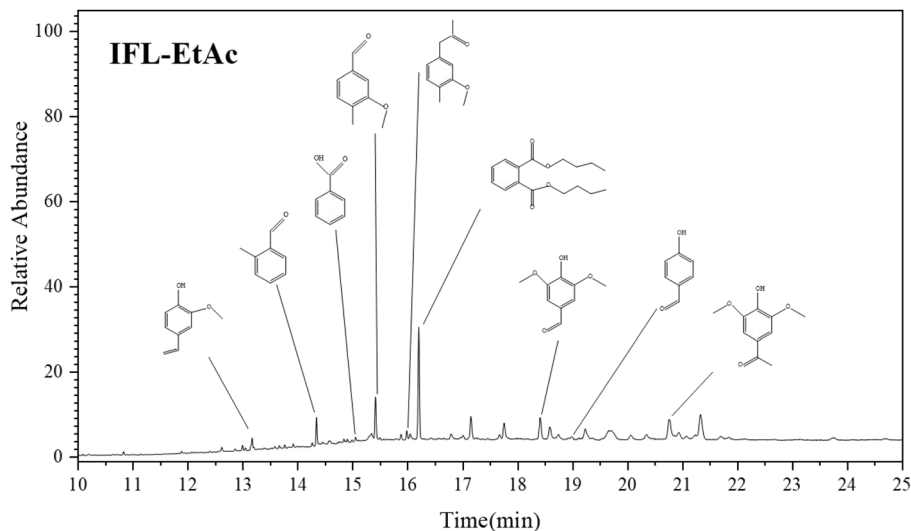
Fig. 4 GC/MS analysis for the aromatic monomers in IFL-EtAc fraction.

which can be attributed to formylation reaction between lignin and FA.[33]

3.4 GC/MS analysis of aromatic monomers

GC/MS analysis was performed to investigate the aromatic monomers of IFL-EtAc extracted by ethyl acetate. As shown in the acquired GC of Fig. 4, nine meaningful aromatic monomers were identified by contrasting with GC/MS databases, including 2-methoxy-4-vinylphenol, 1-(4-hydroxy-3-methoxyphenyl)-ethanone, vanillin, 4-hydroxy-3,5-dimethoxy-benzaldehyde, 1-(4-hydroxy-3,5-dimethoxy phenyl)-ethanone, 2-methyl-benzaldehyde, dibutyl phthalate, and *p*-hydroxy benzaldehyde. It is reasonable to speculate that these aromatic monomers are formed by lignin depolymerization, mostly through β-O-4 cleavage by FA-induced mechanism *via* a formylation, elimination and hydrolysis.[43] It was demonstrated that the proton-

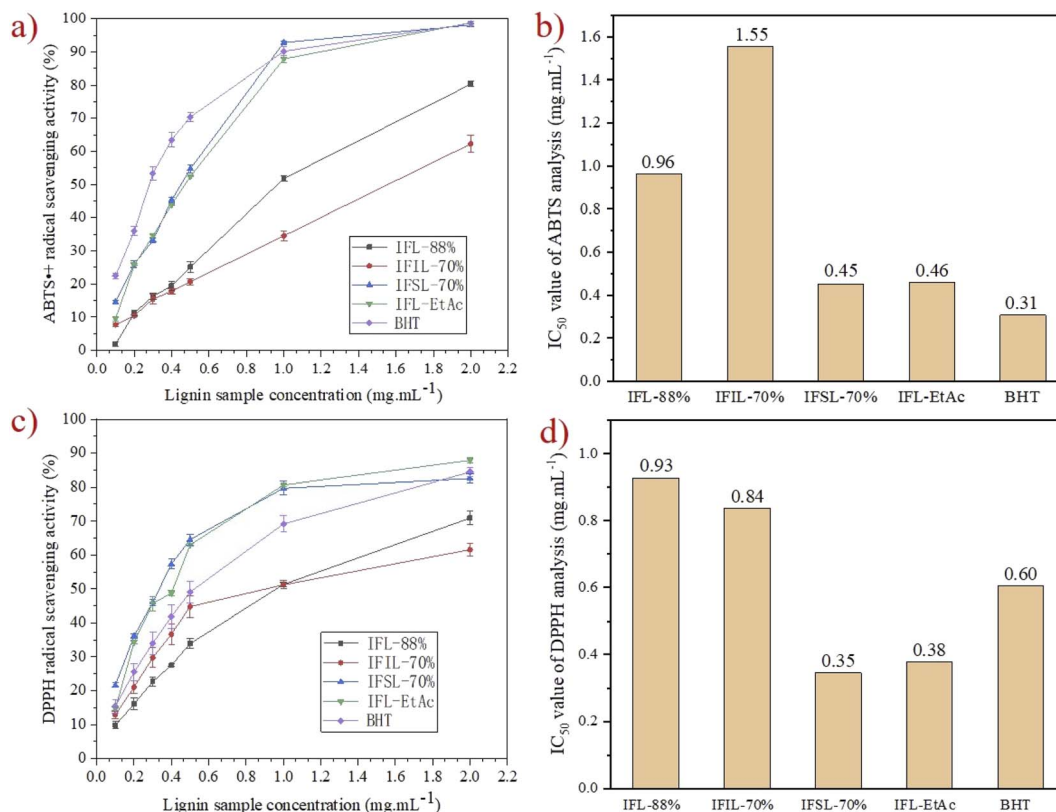**Fig. 5** Antioxidant capacities of ABTS$^{•+}$ and DPPH radical scavenging activity for isolated lignin fractions. (a) ABTS$^{•+}$ radical scavenging activity; (b) IC$_{50}$ of ABTS$^{•+}$ analysis; (c) DPPH radical scavenging activity; (d) IC$_{50}$ of DPPH analysis. BHT was used as the control.

induced elimination of water from the benzylic position could form a carbonium ion at Cα of the side chain under acidic condition, leading to the homolytic cleavage of the β-O-4 substructures.[33,42,44]

3.5 Antioxidant activity analysis of isolated lignin fractions

In order to explore the potential antioxidant capacities of the isolated lignin fractions obtained from sequential two-step formosolv fractionation, $ABTS^{\cdot+}$ and DPPH radical scavenging activities of the isolated lignin fractions were investigated, and the commercial antioxidant, BHT was used as control. The calculated IC_{50} values represent the concentration inhibiting 50% of the initial $ABTS^{\cdot+}$ and DPPH radicals. The results are shown in Fig. 5.

As observation in Fig. 5a, $ABTS^{\cdot+}$ radical scavenging ability of isolated lignin fractions increases with the concentration of lignin fractions. IFL-EtAc and IFSL-70% show the highest $ABTS^{\cdot+}$ activity (99 ± 0.3%) at the concentration of 2.0 mg mL^{-1} among the isolated lignin fractions, even equal to the commercial available antioxidant, BHT (~60%) at the same concentration. Fig. 5b shows the calculated IC_{50} value of $ABTS^{\cdot+}$ analysis of isolated lignin fractions. It can be seen that IFIL-70% has the highest IC_{50} value in $ABTS^{\cdot+}$ analysis, 1.55 mg mL^{-1}, followed by IFL-88% (0.96 mg mL^{-1}), and IFSL-70% and IFL-EtAc has the lowest IC_{50} value, 0.45 and 0.46 mg mL^{-1}, respectively.

As expected, DPPH radical scavenging capability of isolated lignin fractions is also increasing with the concentration of lignin fractions (Fig. 5c). As shown in Fig. 5c, the DPPH radical scavenging activity of the isolated lignin fractions at 2.0 mg mL^{-1} was decreasing by the order of IFL-EtAc (88 ± 0.7%) > IFSL-70% (83 ± 1.4%) > IFIL-70% (71 ± 2.0%) > IFL-88% (62 ± 1.8%). Correspondingly, IFL-88% and IFIL-70% have the calculated IC_{50} value of DPPH analysis, 0.93 mg mL^{-1} and 0.84 mg mL^{-1}, respectively, higher than IFL-EtAc (0.38 mg mL^{-1}) and IFSL-70% (0.35 mg mL^{-1}) (Fig. 5d). Among these isolated lignin fractions, IFL-EtAc and IFSL-70% exhibit the highest antioxidant activity, which is mainly ascribed to the high total phenolic content (Fig. 2d) and reactivity methoxyl groups (Fig. 3). Many researches have demonstrated that phenolic hydroxyl groups can form phenoxy radicals to capture the hydroxyl radicals, and methoxyl groups show a stabilizing effect on the formed phenoxy radicals.[45–48] On the other hand, decrease in M_w, PDI and heterogeneity of lignin can increase its antioxidant capabilities.[3] As seen from Table 1, IFL-EtAc and IFSL-70% have lower M_w (2760 Da and 3123 Da, respectively) and better uniformity PDI (1.5 and 1.6, respectively), which will improve lignin antioxidant activity. These experimental data indicate that IFL-EtAc and IFSL-70% have higher radical scavenging activity than IFIL-70% and IFL-88%.

4 Conclusions

In summary, sequential two-step formosolv fractionation of lignin from biomass could cause lignin depolymerization in accompanied with condensation reaction, leading to different antioxidant activity and structural properties of the isolated lignin fractions. GPC, FTIR, HSQC-NMR, and TGA techniques were employed to characterize the structural properties of the isolated lignin fractions, and nine aromatic monomers are determined by GC/MS. Furthermore, TPC values of the isolated lignin fractions were quantitatively measured by FC method. These structural properties and TPC values were responsible for the $ABTS^{\cdot+}$ and DPPH radical scavenging activity of the isolated lignin fractions. These findings suggest that sequential two-step formosolv fractionation is an efficient approach to upgrade lignin for downstream antioxidant applications.

Author contributions

YL (Yun Liu) completed conceptualization and supervision of the project, wrote and revised the manuscript. XD (Xiaoxia Duan) measured the structural properties of lignin and drafted the manuscript. XW (Xueke Wang) completed lignin isolation and antioxidant activity. JC (Jiangwei Chen) drew the molecular formula and edited the references; GL (Guijiang Liu) drew the graphical abstract.

Conflicts of interest

The authors declare no conflicts of interest.

Acknowledgements

References

1 X. Lu, X. Gu and Y. Shi, A review on lignin antioxidants: their sources, isolations, antioxidant activities and various applications, *Int. J. Biol. Macromol.*, 2022, **210**, 716–741, DOI: **10.1016/j.ijbiomac.2022.04.228**.

2 Y. Sheng, Z. Ma, X. Wang and Y. Han, Ethanol organosolv lignin from different agricultural residues: toward basic structural units and antioxidant activity, *Food Chem.*, 2022, **376**, 131895, DOI: **10.1016/j.foodchem.2021.131895**.

3 T. V. Lourençon, G. G. de Lima, C. S. P. Ribeiro, F. A. Hansel, G. M. Maciel, K. Da Silva, S. M. B. Winnischofer, C. I. B. Muniz and W. L. E. Magalhães, Antioxidant, antibacterial and antitumoural activities of kraft lignin from hardwood fractionated by acid precipitation, *Int. J. Biol. Macromol.*, 2021, **166**, 1535–1542, DOI: **10.1016/j.ijbiomac.2020.11.033**.

4 S. Dapía, V. Santos and J. C. Parajó, Study of formic acid as an agent for biomass fractionation, *Biomass Bioenergy*, 2022, **22**(3), 213–221, DOI: **10.1016/S0961-9534(01)00073-3**.

5 Y. Yu, H. Xu, H. Yu, L. Hu and Y. Liu, Formic acid fractionation towards highly efficient cellulose-derived PdAg bimetallic catalyst for H$_2$ evolution, *Green Energy*

Environ., 2022, **7**(1), 172–183, DOI: **10.1016/j.gee.2020.08.006**.

6 M. Zhang, W. Qi, R. Liu, R. Su, S. Wu and Z. He, Fractionating lignocellulose by formic acid: characterization of major components, *Biomass Bioenergy*, 2010, **34**(4), 525–532, DOI: **10.1016/j.biombioe.2009.12018**.

7 M. Li, P. Yu, S. Li, X. Wu, X. Xiao and J. Bian, Sequential two-step fractionation of lignocellulose with formic acid organosolv followed by alkaline hydrogen peroxide under mild conditions to prepare easily saccharified cellulose and value-added lignin, *Energy Convers. Manag.*, 2017, **148**, 1426–1437, DOI: **10.1016/j.enconman.2017.07.008**.

8 N. Suriyachai, V. Champreda, N. Kraikul, W. Techanan and N. Laosiripojana, Fractionation of lignocellulosic biopolymers from sugarcane bagasse using formic acid-catalyzed organosolv process, *Biotech*, 2018, **8**(5), 221, DOI: **10.1007/s13205-018-1244-9**.

9 C. Jin, M. E. S. Yang, J. Liu, S. Zhang, X. Zhang, K. Sheng and X. Zhang, Corn stover valorization by one-step formic acid fractionation and formylation for 5-hydroxymethylfurfural and high guaiacyl lignin production, *Bioresour. Technol.*, 2020, **299**, 122586, DOI: **10.1016/j.biortech.2019.122586**.

10 H. Qiao, S. Ouyang, J. Shi, Z. Zheng and J. Ouyang, Mild and efficient two-step pretreatment of lignocellulose using formic acid solvent followed by alkaline salt, *Cellulose*, 2021, **28**(3), 1283–1293, DOI: **10.1007/s10570-020-03622-8**.

11 Z. Shao, Y. Fu, P. Wang, Y. Zhang, M. Qin, X. Li and F. Zhang, Modification of the aspen lignin structure during integrated fractionation process of autohydrolysis and formic acid delignification, *Int. J. Biol. Macromol.*, 2020, **165**, 1727–1737, DOI: **10.1016/j.ijbiomac.2020.10.026**.

12 H. V. Halleraker, S. Ghoreishi and T. Barth, Investigating reaction pathways for formic acid and lignin at HTL conditions using 13C-labeled formic acid and 13C NMR, *Results Chem.*, 2020, **2**, 100019, DOI: **10.1016/j.rechem.2019.100019**.

13 U. Shakeel, X. Li, B. Wang, F. Geng, M. S. U. Rehman, K. Zhang and J. Xu, Structural characterizations of lignins extracted under same severity using different acids, *Int. J. Biol. Macromol.*, 2022, **194**, 204–212, DOI: **10.1016/j.ijbiomac.2021.11.171**.

14 C. Xu, R. A. Arancon, J. Labidi and R. Luque, Lignin depolymerisation strategies: towards valuable chemicals and fuels, *Chem. Soc. Rev.*, 2014, **43**(22), 7485–7500, DOI: **10.1039/c4cs00235k**.

15 S. Zhou, Y. Xue, A. Sharma and X. Bai, Lignin Valorization through Thermochemical Conversion: Comparison of Hardwood, Softwood and Herbaceous Lignin, *ACS Sustainable Chem. Eng.*, 2016, **4**(12), 6608–6617, DOI: **10.1021/acssuschemeng.6b01488**.

16 R. Rinaldi, R. Jastrzebski, M. T. Clough, J. Ralph, M. Kennema, P. C. Bruijnincx and B. M. Weckhuysen, Paving the Way for Lignin Valorisation: Recent Advances in Bioengineering, Biorefining and Catalysis, *Angew. Chem., Int. Ed.*, 2016, **55**(29), 8164–8215, DOI: **10.1002/anie.201510351**.

17 X. Yang, Z. Li, L. Li, N. Li, F. Jing, L. Hu and X. Pan, Depolymerization and Demethylation of Kraft Lignin in Molten Salt Hydrate and Applications as an Antioxidant and Metal Ion Scavenger, *J. Agric. Food Chem.*, 2021, **69**(45), 13568–13577, DOI: **10.1021/acs.jafc.1c05759**.

18 Y. Liu, H. Zhou, L. Wang, S. Wang and L. Fan, Improving Saccharomyces cerevisiae growth against lignocellulose-derived inhibitors as well as maximizing ethanol production by a combination proposal of γ-irradiation pretreatment with in situ detoxification, *Chem. Eng. J.*, 2016, **287**, 302–312, DOI: **10.1016/j.cej.2015.10.086**.

19 P. Wang, Y. Fu, Z. Shao, F. Zhang and M. Qin, Structural Changes to Aspen Wood Lignin during Autohydrolysis Pretreatment, *Bioresources*, 2016, **11**(2), 4086–4103, DOI: **10.15376/biores.11.2.4086-4103**.

20 J. L. Wen, S. L. Sun, B. L. Xue and R. C. Sun, Recent Advances in Characterization of Lignin Polymer by Solution-State Nuclear Magnetic Resonance (NMR) Methodology, *Materials*, 2013, **6**(1), 359–391, DOI: **10.3390/ma6010359**.

21 F. H. B. Sosa, D. O. Abranches, A. M. Da Costa Lopes, J. A. P. Coutinho and M. C. Da Costa, Kraft Lignin Solubility and Its Chemical Modification in Deep Eutectic Solvents, *ACS Sustainable Chem. Eng.*, 2020, **8**(50), 18577–18589, DOI: **10.1021/acssuschemeng.0c06655**.

22 S. E. Klein, J. Rumpf, A. Alzagameem, M. Rehahn and M. Schulze, Antioxidant activity of unmodified kraft and organosolv lignins to be used as sustainable components for polyurethane coatings, *J. Coat. Technol. Res.*, 2019, **16**(6), 1543–1552, DOI: **10.1007/s11998-019-00201-w**.

23 K. R. Aadil, A. Barapatre, S. Sahu, H. Jha and B. N. Tiwary, Free radical scavenging activity and reducing power of Acacia nilotica wood lignin, *Int. J. Biol. Macromol.*, 2014, **67**, 220–227, DOI: **10.1016/j.ijbiomac.2014.03.040**.

24 X. Wei, Y. Liu, Y. Luo, Z. Shen, S. Wang, M. Li and L. Zhang, Effect of organosolv extraction on the structure and antioxidant activity of eucalyptus kraft lignin, *Int. J. Biol. Macromol.*, 2021, **187**, 462–470, DOI: **10.1016/j.ijbiomac.2021.07.082**.

25 M. Zhang, W. Qi, R. Liu, R. Su, S. Wu and Z. He, Fractionating lignocellulose by formic acid: characterization of major components, *Biomass Bioenergy*, 2010, **34**(4), 525–532, DOI: **10.1016/j.biombioe.2009.12.018**.

26 Q. Ma, L. Wang, H. Zhai and H. Ren, Lignin dissolution model in formic acid–acetic acid–water systems based on lignin chemical structure, *Int. J. Biol. Macromol.*, 2021, **182**, 51–58, DOI: **10.1016/j.ijbiomac.2021.03.179**.

27 Q. Ma, Z. Li, L. Guo, H. Zhai and H. Ren, Formation of high carbohydrate and acylation condensed lignin from formic acid-acetic acid-H$_2$O biorefinery of corn stalk rind, *Ind. Crops Prod.*, 2020, **161**, 113165, DOI: **10.1016/j.indcrop.2020.113165**.

28 J. Zhang, H. Deng, L. Lin, Y. Sun, C. Pan and S. Liu, Isolation and characterization of wheat straw lignin with a formic acid process, *Bioresour. Technol.*, 2010, **101**(7), 2311–2316, DOI: **10.1016/j.biortech.2009.11.037**.

29 Y. Zhang, Q. Hou, Y. Fu, C. Xu, A. I. Smeds, S. Willför and M. Qin, One-Step Fractionation of the Main Components

of Bamboo by Formic Acid-based Organosolv Process Under Pressure, *J. Wood Chem. Technol.*, 2018, **38**(3), 170–182, DOI: **10.1080/02773813.2017.1388823**.

30 M. Rana, T. Nshizirungu and J. Park, Synergistic effect of water-ethanol-formic acid for the depolymerization of industrial waste (black liquor) lignin to phenolic monomers, *Biomass Bioenergy*, 2021, **153**, 106204, DOI: **10.1016/j.biombioe.2021.106204**.

31 X. Yang, Z. Li, L. Li, N. Li, F. Jing, L. Hu and X. Pan, Depolymerization and Demethylation of Kraft Lignin in Molten Salt Hydrate and Applications as an Antioxidant and Metal Ion Scavenger, *J. Agric. Food Chem.*, 2021, **69**(45), 13568–13577, DOI: **10.1021/acs.jafc.1c05759**.

32 H. Cao, R. Liu, B. Li, Y. Wu, K. Wang, Y. Yang and P. Qin, Biobased rigid polyurethane foam using gradient acid precipitated lignin from the black liquor: Revealing the relationship between lignin structural features and polyurethane performances, *Ind. Crops Prod.*, 2021, **177**, 114480, DOI: **10.1016/j.indcrop.2021.114480**.

33 Z. Shao, Y. Fu, P. Wang, Y. Zhang, M. Qin, X. Li and F. Zhang, Modification of the aspen lignin structure during integrated fractionation process of autohydrolysis and formic acid delignification, *Int. J. Biol. Macromol.*, 2020, **165**, 1727–1737, DOI: **10.1016/j.ijbiomac.2020.10.026**.

34 M. Wądrzyk, R. Janus, M. Lewandowski and A. Magdziarz, On mechanism of lignin decomposition – investigation using microscale techniques: Py-GC-MS, Py-FT-IR and TGA, *Renewable Energy*, 2021, **177**, 942–952, DOI: **10.1016/j.renene.2021.06.006**.

35 J. Kim, S. Oh, H. Hwang, U. Kim and J. W. Choi, Structural features and thermal degradation properties of various lignin macromolecules obtained from poplar wood (*Populus albaglandulosa*), *Polym. Degrad. Stab.*, 2013, **98**(9), 1671–1678, DOI: **10.1016/j.polymdegradstab.2013.06.008**.

36 C. Jin, M. Yang, E. Shuang, J. Liu, S. Zhang, X. Zhang and X. Zhang, Corn stover valorization by one-step formic acid fractionation and formylation for 5-hydroxymethylfurfural and high guaiacyl lignin production, *Bioresour. Technol.*, 2020, **299**, 122586, DOI: **10.1016/j.biortech.2019.122586**.

37 X. Zhong, R. Yuan, B. Zhang, B. Wang, Y. Chu and Z. Wang, Full fractionation of cellulose, hemicellulose, and lignin in pith-leaf containing corn stover by one-step treatment using aqueous formic acid, *Ind. Crops Prod.*, 2021, **172**, 113962, DOI: **10.1016/j.indcrop.2021.113962**.

38 X. Zhong, R. Yuan, B. Zhang, B. Wang, Y. Chu and Z. Wang, High β-O-4 polymeric lignin and oligomeric phenols from flow-through fractionation of wheat straw using recyclable aqueous formic acid, *Ind. Crops Prod.*, 2021, **172**, 113962, DOI: **10.1016/j.indcrop.2021.113962**.

39 J. Zeng, G. L. Helms, X. Gao and S. Chen, Quantification of wheat straw lignin structure by comprehensive NMR analysis, *J. Agric. Food Chem.*, 2013, **61**(46), 10848–10857, DOI: **10.1021/jf4030486**.

40 H. Zhou, R. Zhang, W. Zhan, L. Wang, L. Guo and Y. Liu, High biomass loadings of 40 wt% for efficient fractionation in biorefineries with an aqueous solvent system without adding adscititious catalyst, *Green Chem.*, 2016, **18**(22), 6108–6114, DOI: **10.1039/C6GC02225A**.

41 M. M. Abu-Omar, K. Barta, G. T. Beckham, J. Luterbacher, J. Ralph and R. Rinaldi, National Renewable Energy Lab. NREL, G. C. U. S. Guidelines for performing lignin-first biorefining, *Energy Environ. Sci.*, 2021, **14**(1), 262–292, DOI: **10.1039/d0ee02870c**.

42 S. Hong, X. Shen, Z. Xue, Z. Sun and T. Yuan, Structure-function relationships of deep eutectic solvents for lignin extraction and chemical transformation, *Green Chem.*, 2020, **22**(21), 7219–7232, DOI: **10.1039/d0gc02439b**.

43 M. Oregui-Bengoechea, I. Gandarias, P. L. Arias and T. Barth, Unraveling the Role of Formic Acid and the Type of Solvent in the Catalytic Conversion of Lignin: A Holistic Approach, *ChemSusChem*, 2017, **10**(4), 754–766, DOI: **10.1002/cssc.201601410**.

44 K. Wang, H. Yang, X. Yao, F. Xu and R. Sun, Structural transformation of hemicelluloses and lignin from triploid poplar during acid-pretreatment based biorefinery process, *Bioresour. Technol.*, 2012, **116**, 99–106, DOI: **10.1016/j.biortech.2012.04.028**.

45 X. Wei, Y. Liu, Y. Luo, Z. Shen, S. Wang, M. Li and L. Zhang, Effect of organosolv extraction on the structure and antioxidant activity of eucalyptus kraft lignin, *Int. J. Biol. Macromol.*, 2021, **187**, 462–470, DOI: **10.1016/j.ijbiomac.2021.07.082**.

46 P. Jevgenija, L. Maris, D. Tatiana, L. Liga, J. Vilhelmina and T. Galina, Antioxidant activity of various lignins and lignin-related phenylpropanoid units with high and low molecular weight, *Holzforschung*, 2015, **69**(6), 795–805, DOI: **10.1515/hf-2014-0280**.

47 X. Meng, A. Parikh, B. Seemala, R. Kumar, Y. Pu, P. Christopher and A. J. Ragauskas, Chemical transformations of poplar lignin during cosolvent enhanced lignocellulosic fractionation process, *ACS Sustainable Chem. Eng.*, 2018, **6**(7), 8711–8718, DOI: **10.1021/acssuschemeng.8b01028**.

48 A. García, A. Toledano, M. Á. Andrés and J. Labidi, Study of the antioxidant capacity of Miscanthus sinensis lignins, *Process Biochem.*, 2010, **45**(6), 935–940, DOI: **10.1016/j.procbio.2010.02.015**.